Diffractive scintillation studies of EPTA pulsars

南阳

刘雨兰（中国科学院国家天文台博士后）

合作导师 - 姜鹏

2023年07月04日

1、Diffractive scintillation

2、Methods and Applications

3、Periodic interstellar scintillation variations

4、Current works

Diffractive scintillation

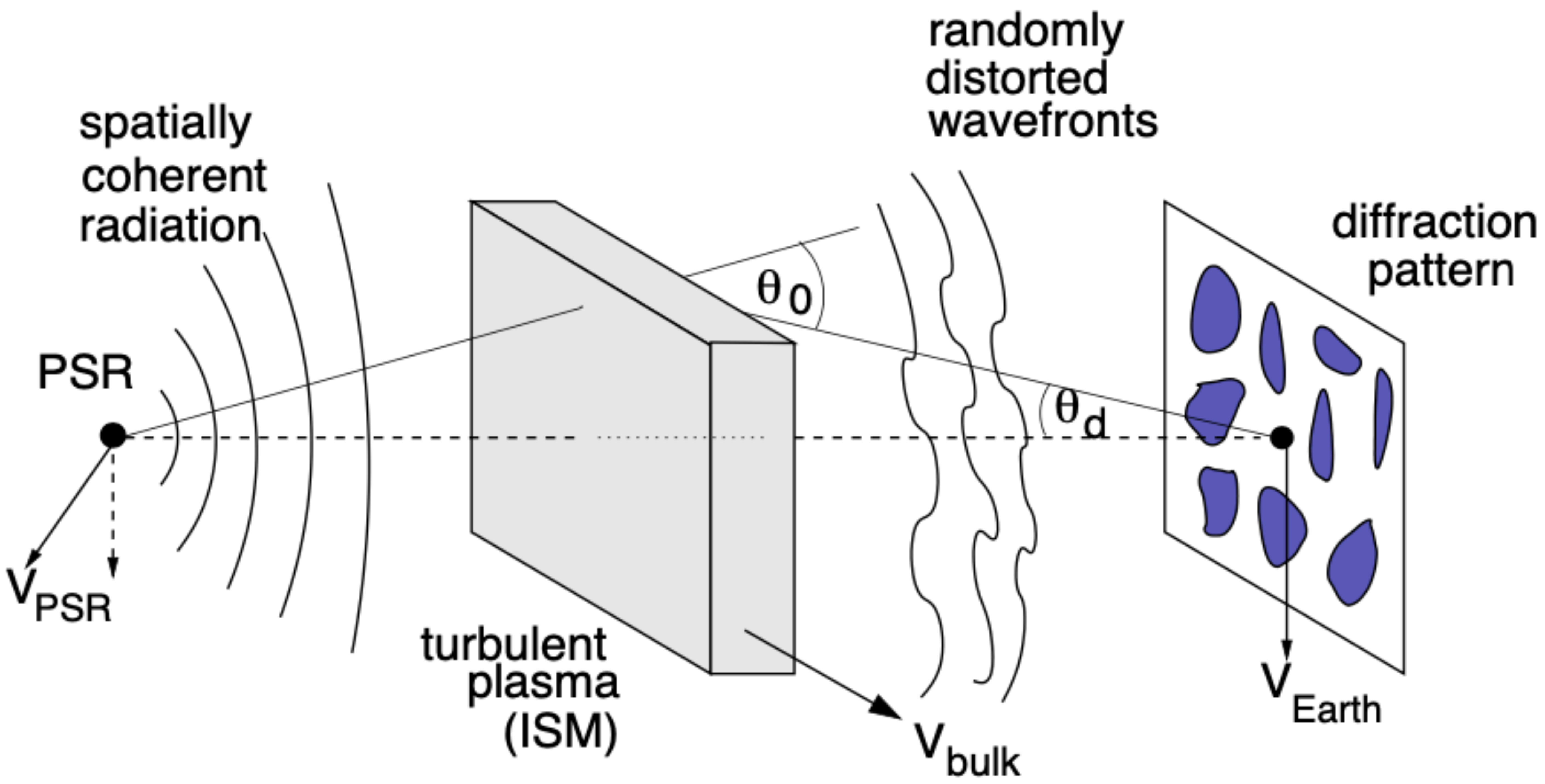

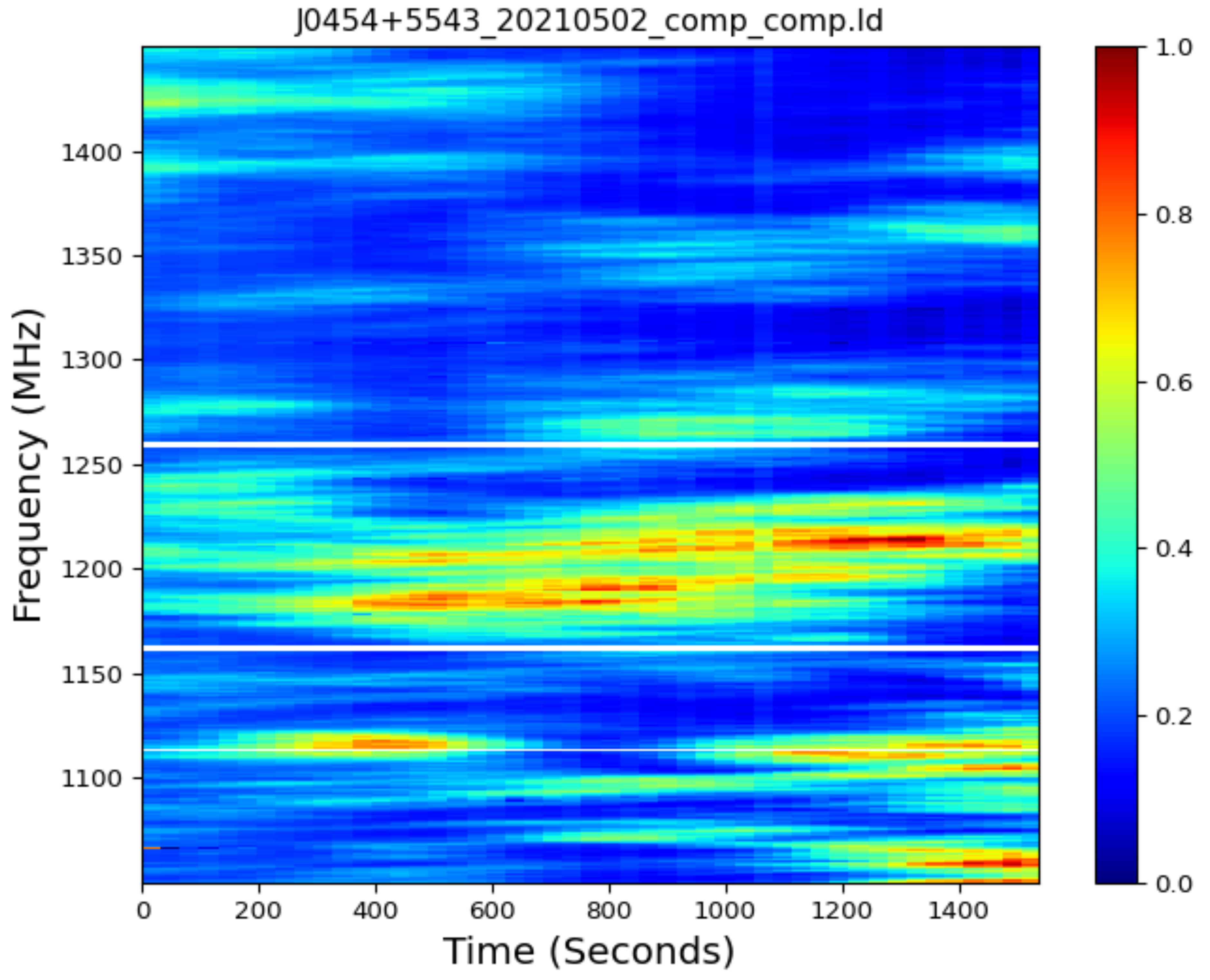

Methods

$$\mathrm{ACF}(\Delta f, \Delta t) = \frac{R(\Delta f, \Delta t)}{R(0,0)}$$

$$R(\Delta f, \Delta t) = \; <\Delta I(f,t) \cdot \Delta I(f + \Delta f, t + \Delta t)>$$

$$\mathrm{ACF}(\nu = 0, \tau) = \exp(-a \cdot \tau^2),$$
$$\mathrm{ACF}(\nu, \tau = 0) = \exp(-b \cdot \nu^2).$$

Scintillation timescale: $\tau_\mathrm{d} = \sqrt{\frac{1}{a}},$

Scintillation bandwidth: $\nu_\mathrm{d} = \sqrt{\frac{\ln 2}{b}}.$

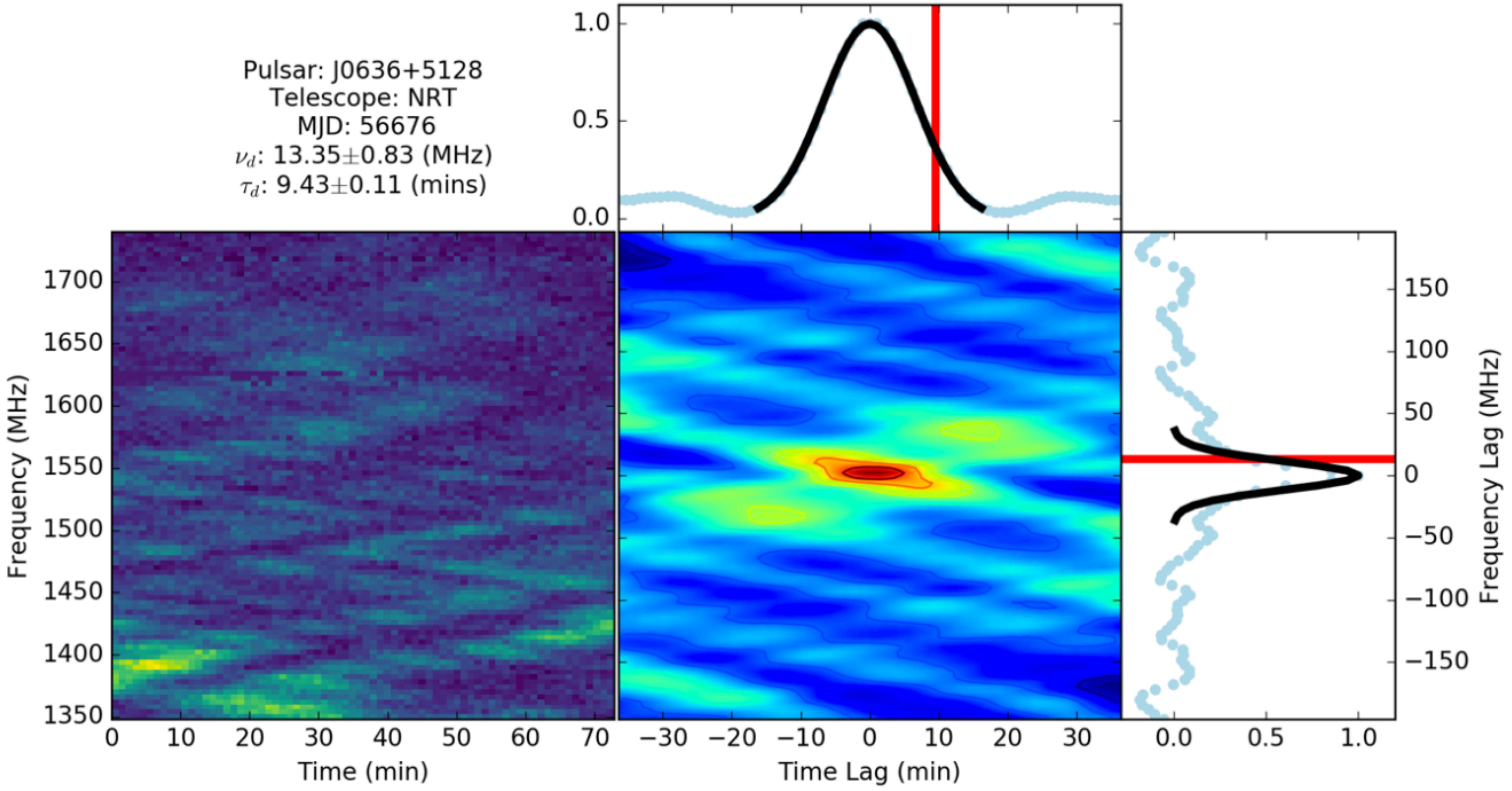

Applications

(1) Study the IISM nature

$$\nu_d \propto f^{\alpha_{\nu_d}} \qquad \alpha_{\nu_d} = 4.4$$

(2) Improve timing precision

$$2\pi\nu_d\tau_{st} = C_1$$

(3) Constrain the scattering screen distance

(4) Constrain the pulsar proper motion

$$\tau_d = \frac{l_d}{V_{ISS}}$$

(5) Probe the pulsar orbital information

$$V_{ISS} = V_{eff}/s$$

(*Lyne, A. G. 1984, Natur, 310, 300*)

…

$$V_{eff}(s) = sV_E + (1-s)(V_p + V_\mu) - V_{IISM}(s),$$

Periodic interstellar scintillation variations of PSRs J0613−0200 and J0636+5128

$$V_{\rm ISS} = A_{\rm ISS}\frac{\sqrt{D\nu_{\rm d}}}{f\tau_{\rm d}},$$

$$V_{\rm ISS} = |V_{\rm eff}|\frac{D}{D-D_s}$$

$$\frac{\sqrt{\nu_{\rm d}}}{f\tau_{\rm d}} \equiv Y = \frac{|V_{\rm eff}|}{A_{\rm ISS}}\frac{\sqrt{D}}{D-D_s}$$

$$V_{\rm eff} = \frac{D-D_s}{D}V_{\rm E} + \frac{D_s}{D}(V_{\rm p}+V_{\mu}) - V_{\rm IISM},$$

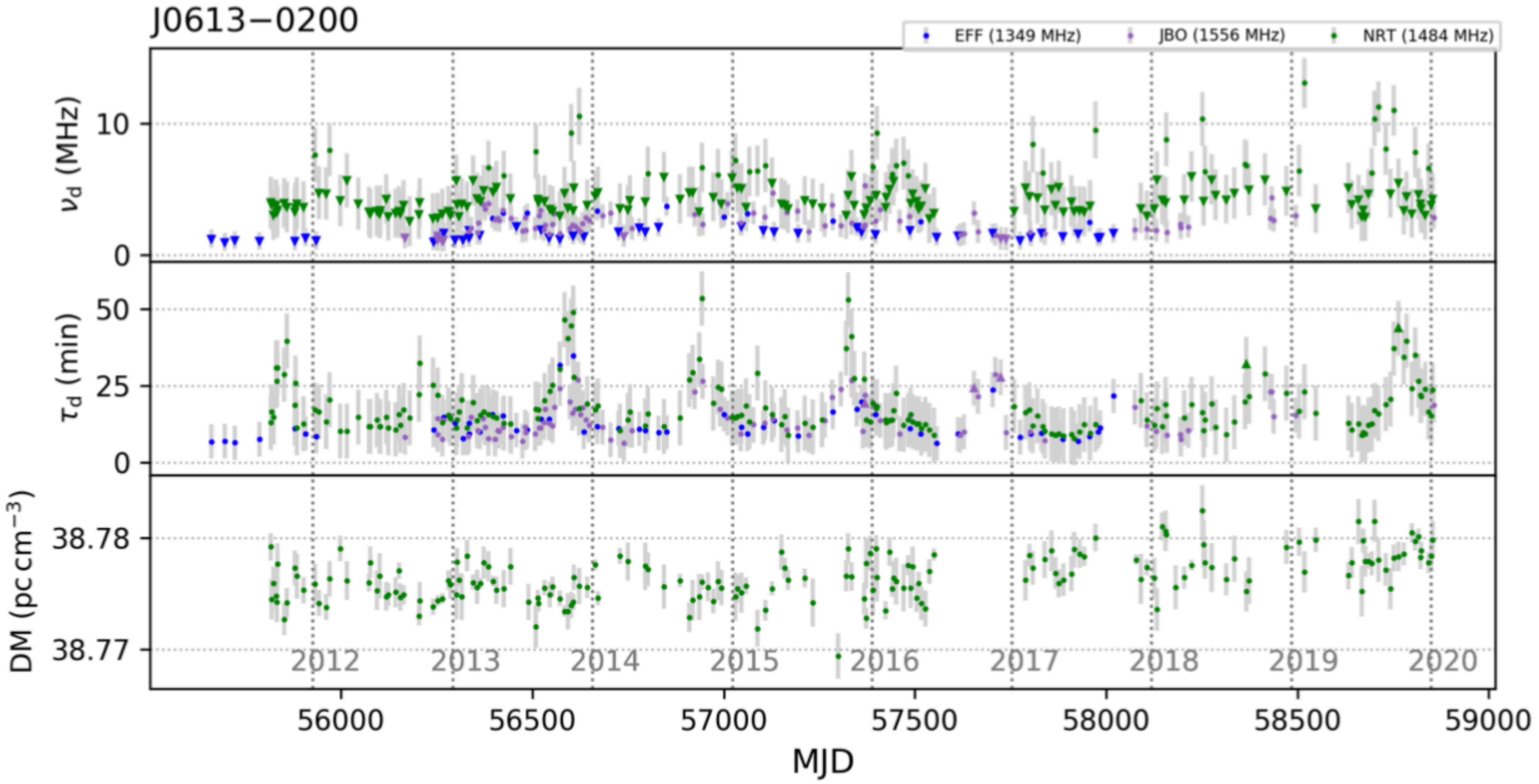

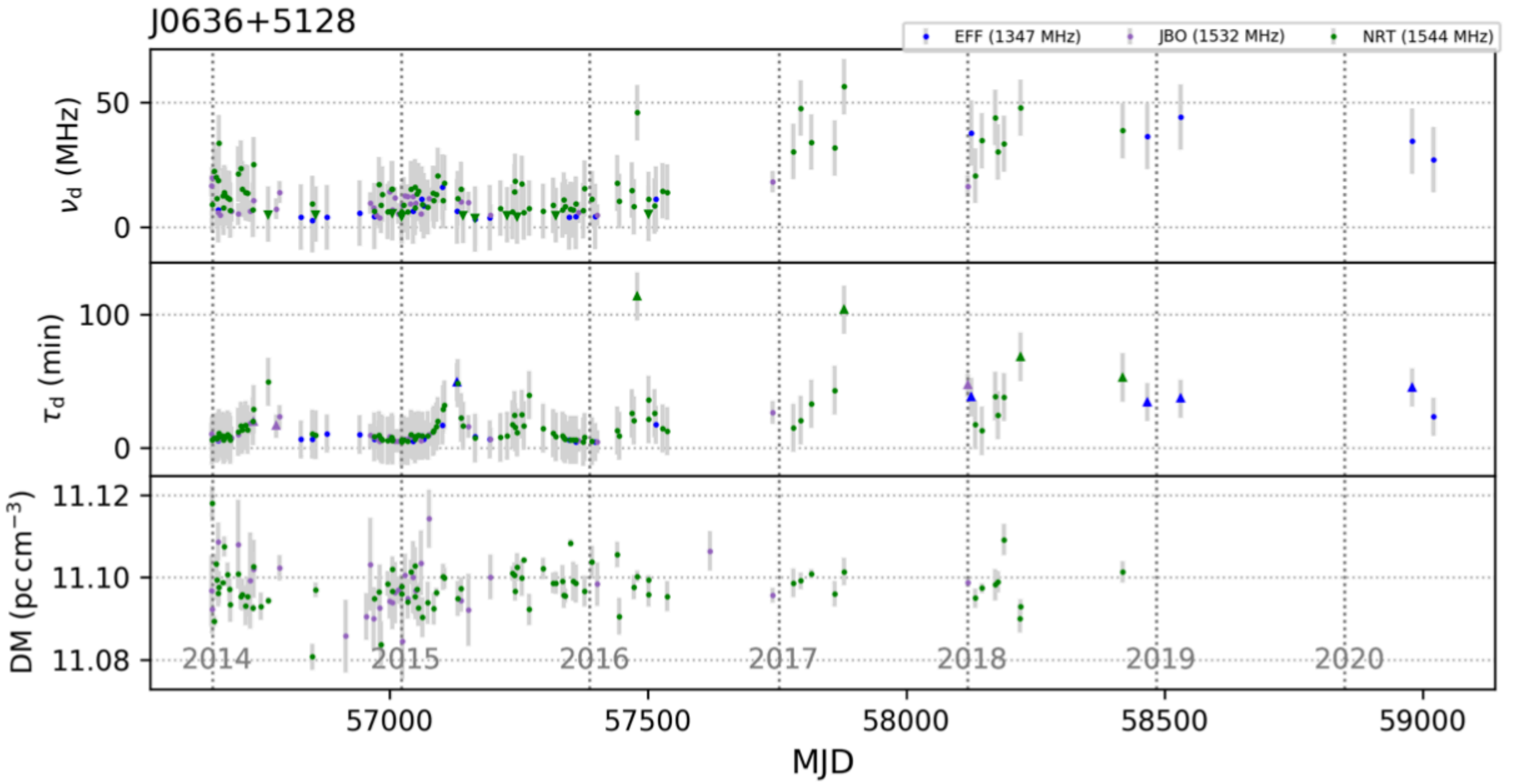

Scattering model

- Uniform
- Thin screen
  - Isotropic
  - Anisotropic
    - Mildly anisotropic scattering
    - Extremely anisotropic scattering

Mildly anisotropic scattering

$$|V_{\rm eff}| = \sqrt{aV^2_{\rm eff,\alpha} + bV^2_{\rm eff,\delta} + cV_{\rm eff,\alpha}V_{\rm eff,\delta}},$$

$$V_{\rm eff,\alpha} = \frac{D-D_s}{D}V_{\rm E,\alpha} + \frac{D_s}{D}(V_{\rm p,\alpha} + V_{\mu,\alpha}) - V_{\rm IISM,\alpha},$$

$$V_{\rm eff,\delta} = \frac{D-D_s}{D}V_{\rm E,\delta} + \frac{D_s}{D}(V_{\rm p,\delta} + V_{\mu,\delta}) - V_{\rm IISM,\delta},$$

$$a = [1 - R\cos(2\psi)] / \sqrt{1-R^2},$$

$$b = [1 + R\cos(2\psi)] / \sqrt{1-R^2},$$

$$c = -2R\sin(2\psi)/ \sqrt{1-R^2},$$

$$A_{\rm ISS} = 2.78\sqrt{(A_r + 1/A_r)/2}\sqrt{2D_s/(D-D_s)} \times 10^4.$$

Extremely anisotropic scattering

$$|V_{\rm eff}| = \left|\sqrt{aV^2_{\rm eff,\alpha} + bV^2_{\rm eff,\delta} + cV_{\rm eff,\alpha}V_{\rm eff,\delta}} - V_{\rm IISM}\right|,$$

$$V_{\rm eff,\alpha} = \frac{D-D_s}{D}V_{\rm E,\alpha} + \frac{D_s}{D}(V_{\rm p,\alpha} + V_{\mu,\alpha}),$$

$$V_{\rm eff,\delta} = \frac{D-D_s}{D}V_{\rm E,\delta} + \frac{D_s}{D}(V_{\rm p,\delta} + V_{\mu,\delta}),$$

$$a = \cos\psi^2,$$

$$b = \sin\psi^2,$$

$$c = -2\sin\psi\cos\psi.$$

$$A_{\rm ISS} = K\sqrt{2D_s/(D-D_s)} \times 10^4$$

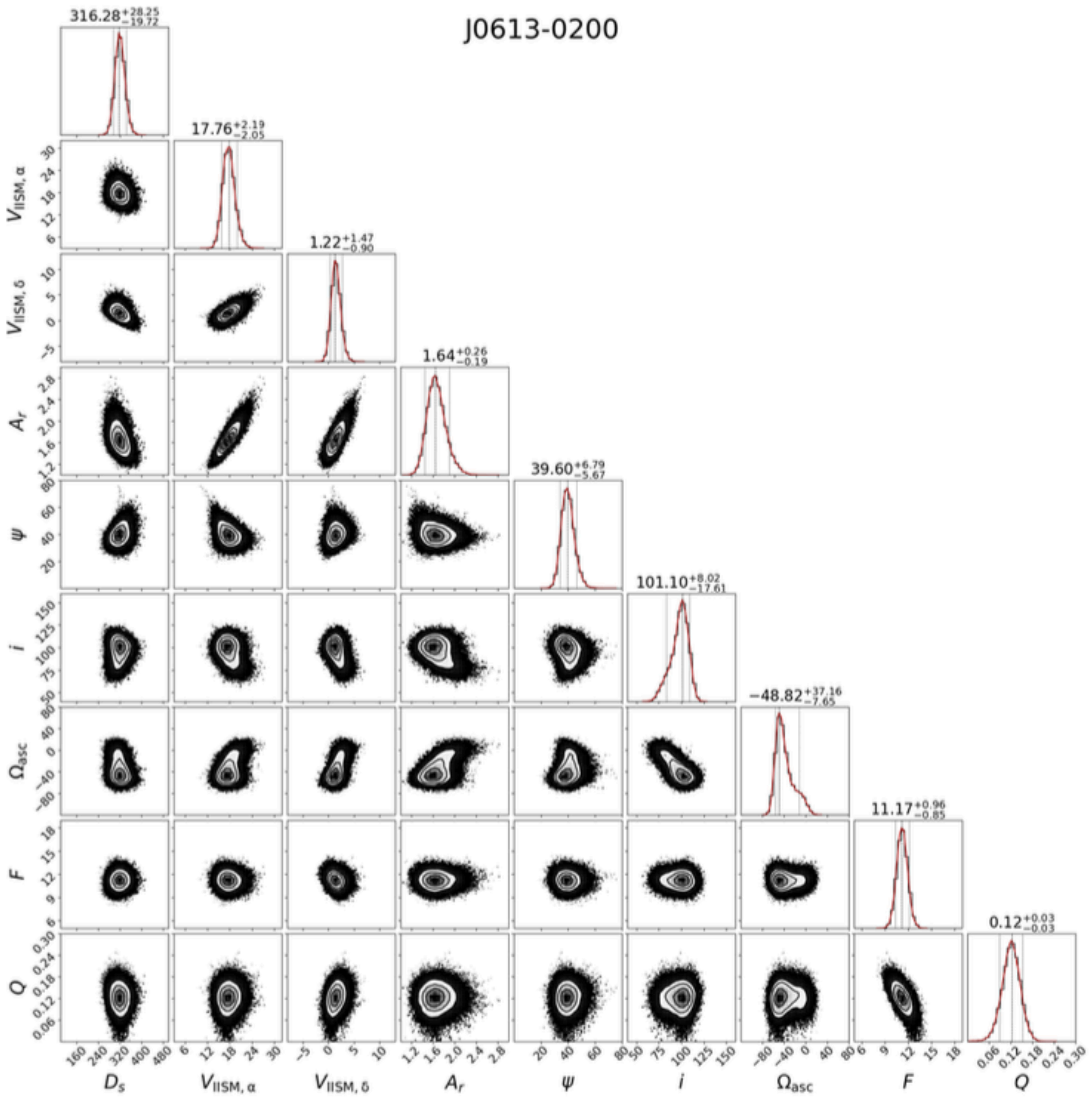

Figure 2 The posterior probability distributions of all fitted parameters for PSR J0613−0200. In the 1-D histograms, the red lines are the kernel-density mate smoothed version of the distributions, the vertical dashed lines indicate the 10% fractional quantiles, the most likely value and 90% fractional quant The most likely value and the upper/lower errors are presented in the top of 1-D histograms. Factors F and Q are the noise parameters EFAC and EQU respectively. The factor Q is magnified a thousand, and it's actually on the order of 10^{-3}, the same as Y.

Mildly anisotropic scattering

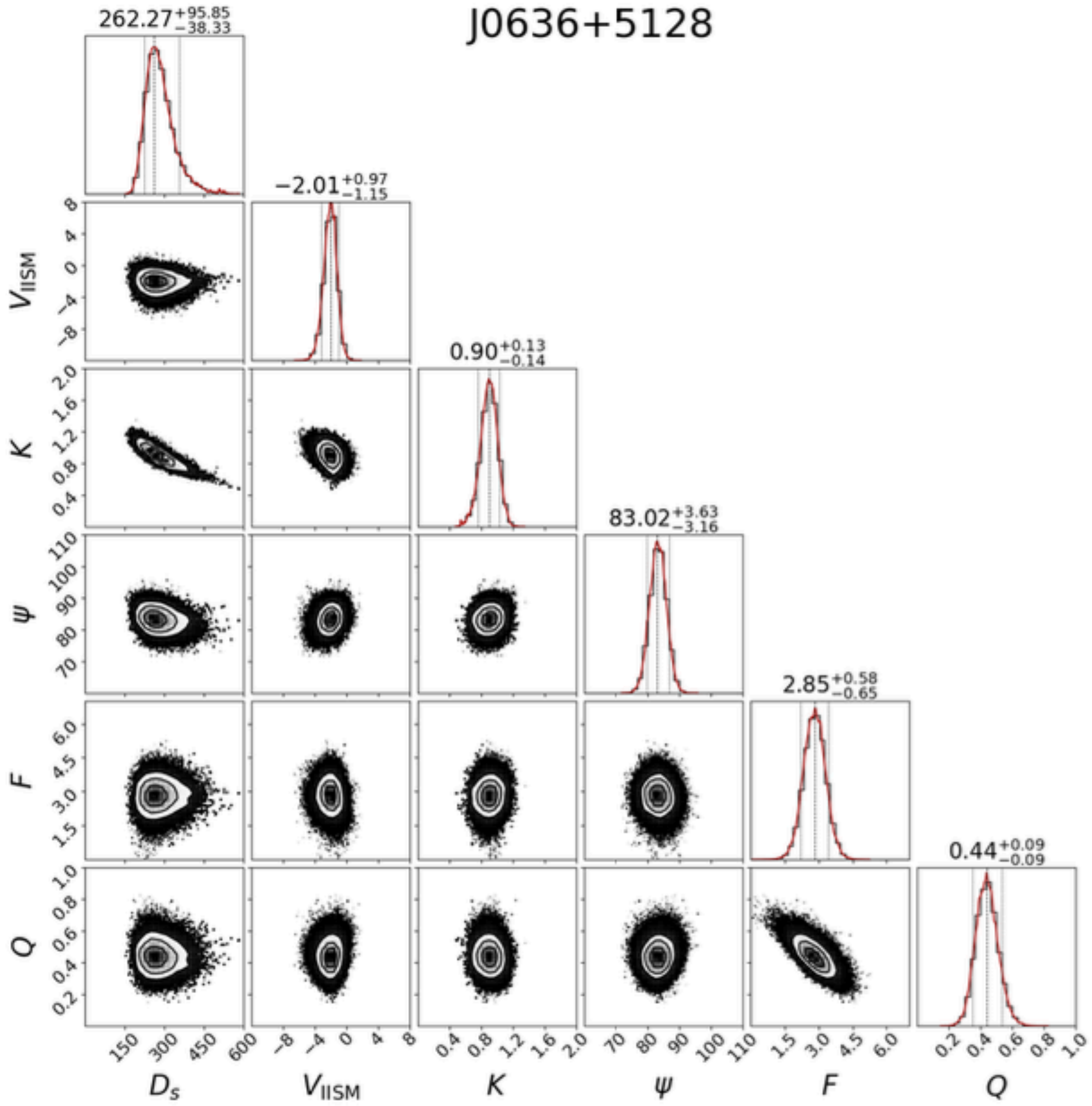

Figure 3 The posterior probability distributions of all fitted parameters for PSR J0636+5128.

Extremely anisotropic scattering

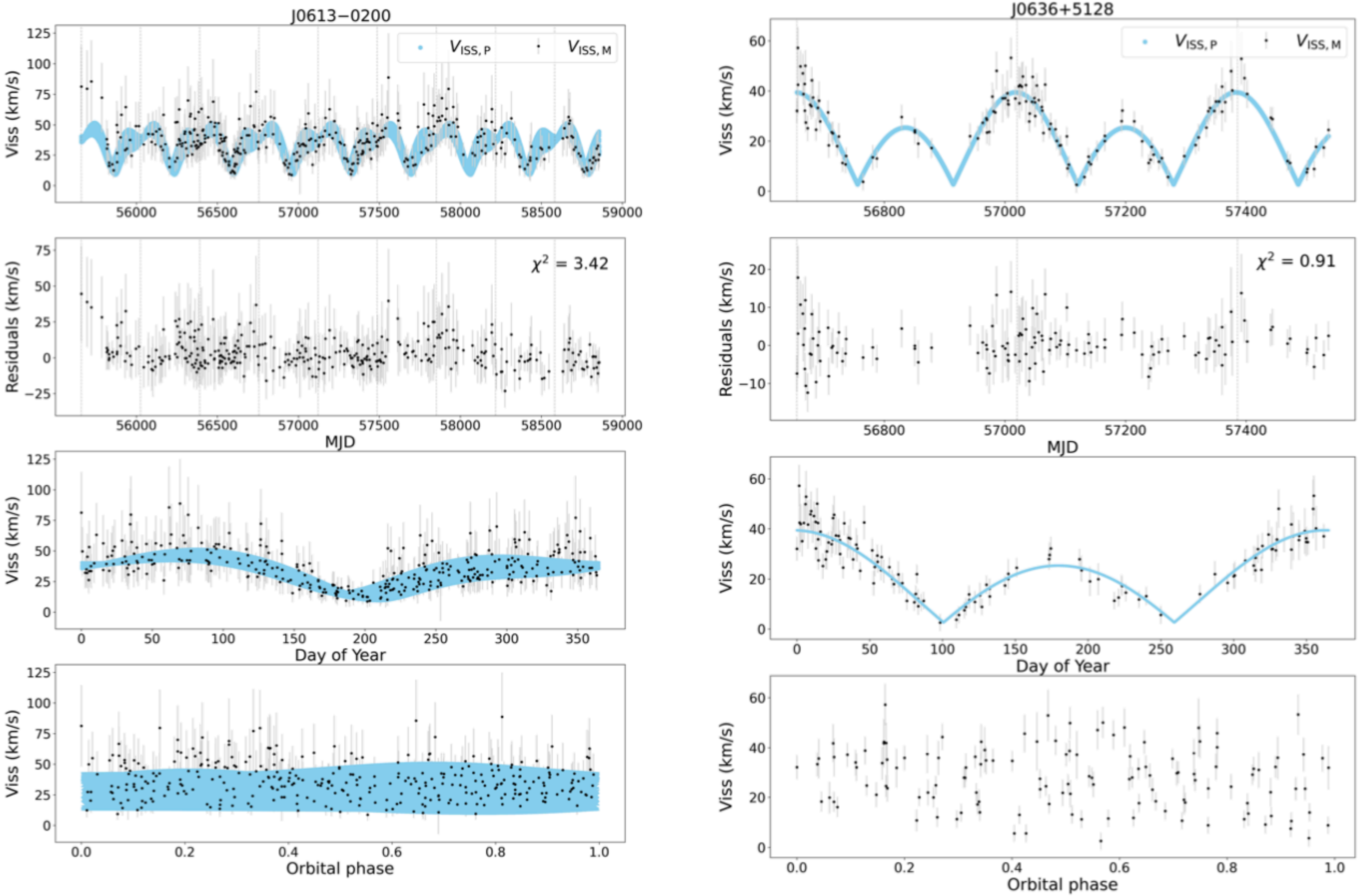

J0613−0200
J0636+5128
$V_{ISS,P}$
$V_{ISS,M}$
Viss (km/s)
Residuals (km/s)
χ^2 = 3.42
χ^2 = 0.91
MJD
Day of Year
Orbital phase

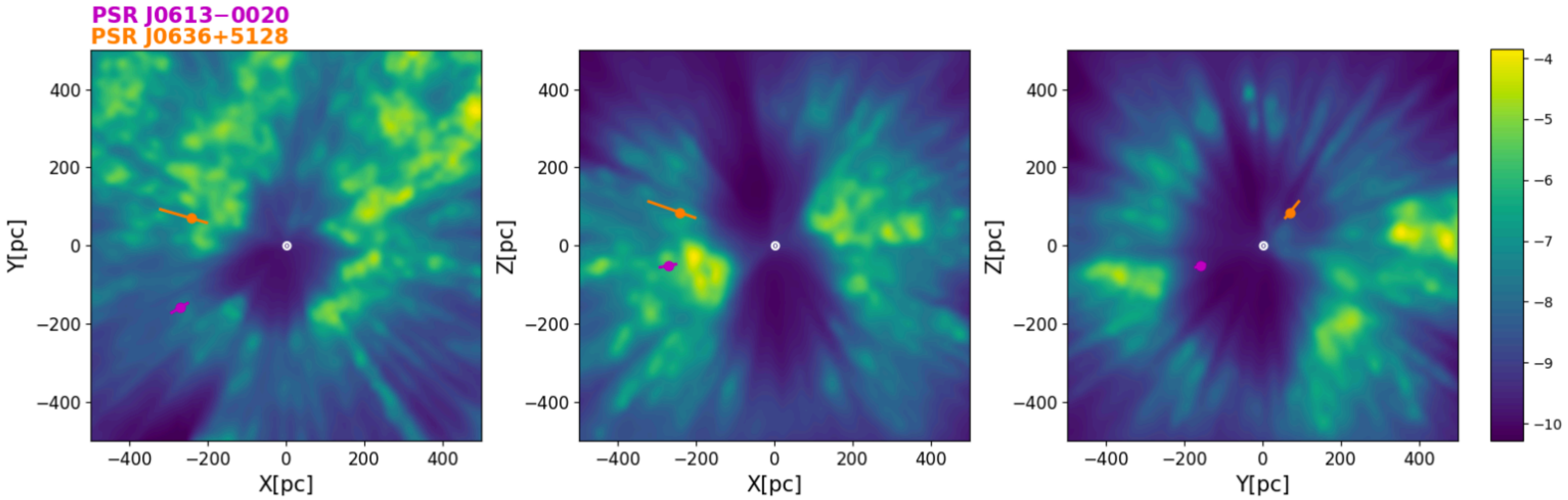

Figure 6 Scintillation screen position on three crosscuts (XY, XZ and YZ planes) of the 3D dust extinction map from Lallement et al. 2019 [45]. The X axis points from the Sun (the circle dot) to the Galactic center, the Y axis points towards $l = 90°$ and the Z axis points to the North Galactic pole at Galactic latitude $b = 90°$. The colour scale shows $\log(A'_v)$ and indicates the gas density, where A'_v is the differential extinction in units of magnitude per parsec.

316^{+28}_{-20} pc and 262^{+96}_{-38} pc

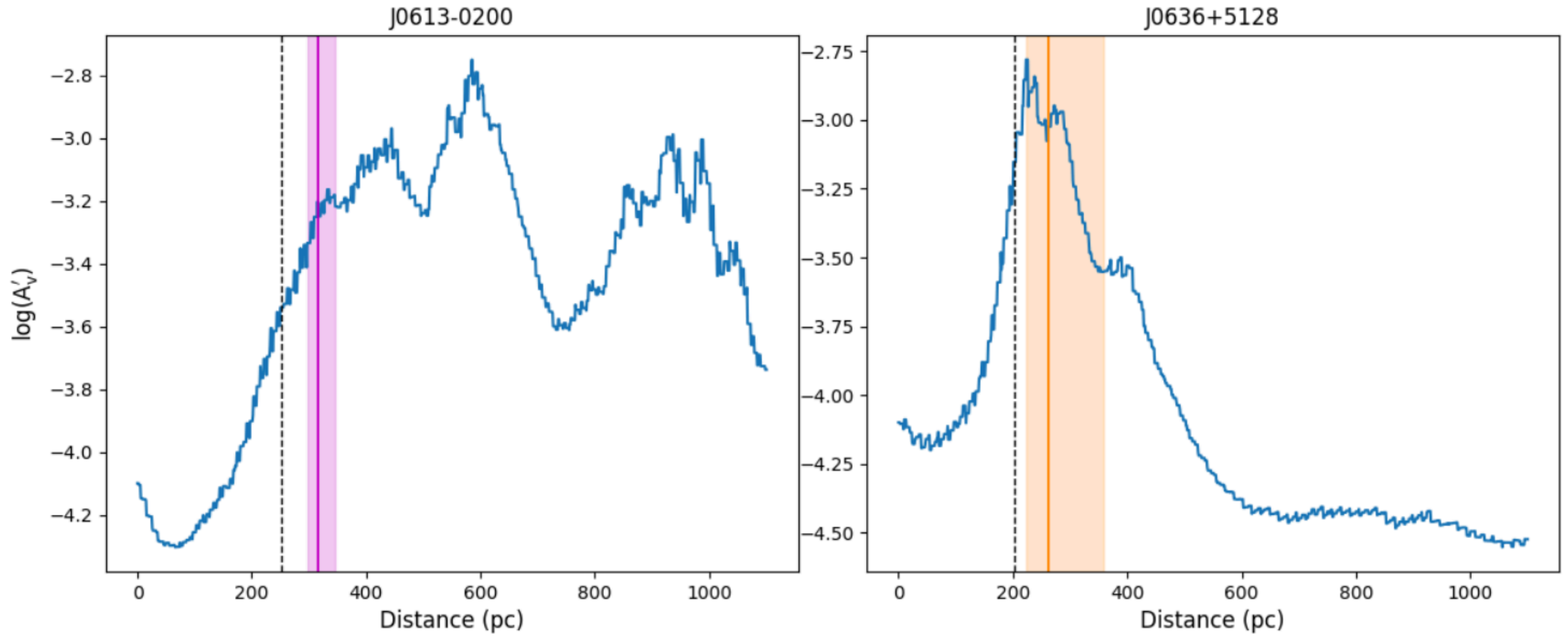

Figure 7 The gas density distribution along the line of sight to two pulsars, from the 3D dust extinction map of Lallement et al. 2019 [45]. The coloured vertical lines denote the estimated position of the scattering screen for each pulsar, while the lighter shades of the vertical lines indicate the uncertainty range of the scintillation screen positions. The dashed black vertical lines indicate positions of the inner local bubble surface on the line of sight to each pulsar.

$$\Omega_{asc} = -48^{+36}_{-9} \text{ degrees}$$

In our modelling, the inclination angle i of PSR J0613−0200 is 101^{+8}_{-18} degrees, the $\sin(i)$ is $0.98^{+0.02}_{-0.03}$

Current works

LAPUDA, LAconic Program Units for pulsar Data Analysis：https://github.com/lujig/lapuda)

LAPUDA

LAPUDA: LAconic Program Units for pulsar Data Analysis

Table of Contents

- Background
- Install
- Usage
- Maintainers
- Contributing
  - Contributors
- License

Thanks